MOLECULAR AND CELLULAR BIOLOGY, Mar. 1996, p. 800–809 Vol. 16, No. 3
0270-7306/96/$04.00+0

Inhibition of v-Mos Kinase Activity by Protein Kinase A

YANDAN YANG, CHRISTINE H. HERRMANN,† RALPH B. ARLINGHAUS, AND BALRAJ SINGH*

Department of Molecular Pathology, The University of Texas M. D. Anderson Cancer Center, Houston, Texas 77030

Received 7 August 1995/Returned for modification 27 September 1995/Accepted 30 November 1995

We investigated the effect of cyclic AMP-dependent protein kinase (PKA) on v-Mos kinase activity. Increase in PKA activity in vivo brought about either by forskolin treatment or by overexpression of the PKA catalytic subunit resulted in a significant inhibition of v-Mos kinase activity. The purified PKA catalytic subunit was able to phosphorylate recombinant p37$^{v\text{-}mos}$ in vitro, suggesting that the mechanism of in vivo inhibition of v-Mos kinase involves direct phosphorylation by PKA. Combined tryptic phosphopeptide two-dimensional mapping analysis and in vitro mutagenesis studies indicated that Ser-56 is the major in vivo phosphorylation site on v-Mos. In vivo phosphorylation at Ser-56 correlated with slower migration of the v-Mos protein during sodium dodecyl sulfate-polyacrylamide gel electrophoresis. However, even though Ser-56 was phosphorylated by PKA, this phosphorylation was not involved in the inhibition of v-Mos kinase. The alanine-for-serine substitution at residue 56 did not affect the ability of v-Mos to autophosphorylate in vitro or, more importantly, to activate MEK1 in transformed NIH 3T3 cells. We identified Ser-263 as the residue that is normally phosphorylated at a very low level but whose phosphorylation is dramatically increased upon forskolin treatment. Consistent with the inhibitory role of Ser-263 phosphorylation, the Ala-263 mutant of v-Mos was not inhibited by forskolin treatment. From our results, we propose that the known inhibitory role of PKA in the initiation of oocyte maturation in mice could be explained at least in part by its inhibition of Mos kinase.

The v-*mos* gene of the Moloney murine sarcoma virus (Mo-MuSV) encodes a serine/threonine protein kinase (32). Mutagenesis studies have shown that the protein kinase function of v-Mos correlates with its biological activity (55). The cellular *mos* gene product (c-Mos) is required for the initiation of meiosis I and II and, as a part of the cytostatic factor, is also responsible for cell cycle arrest of the unfertilized egg at meiotic metaphase II (14, 25, 39, 41, 45, 46, 63). Significantly, v-*mos* and c-*mos* gene products can substitute for each other in cellular transformation functions, induction of meiotic maturation, and cell cycle arrest (18). This implies that both v-Mos and c-Mos are able to recognize the substrates that are relevant for cellular transformation as well for meiotic maturation. Furthermore, since both v-Mos and c-Mos colocalize with microtubules (7, 65), they may be regulated by similar mechanisms.

Our previous studies have shown that phosphorylation plays an important role in the activation of v-Mos kinase (reviewed in reference 54). Specifically, the protein kinase C (PKC) pathway and p34^{cdc2} kinase are involved in the activation of v-Mos kinase (2, 6, 28). In the study reported here, we examined the role of cyclic AMP (cAMP)-dependent protein kinase (PKA) in the regulation of v-Mos protein kinase. This study was prompted by the observation in various laboratories that PKA plays a major inhibitory role in the initiation of oocyte maturation in both frogs and mice (8, 29, 47, 48, 60). Here we report that an increase in PKA activity leads to inhibition of v-Mos kinase activity. Further studies involving in vitro phosphorylation of v-Mos by PKA and tryptic phosphopeptide analysis indicated that v-Mos kinase inhibition may be due to direct phosphorylation by PKA. This is the first report on the inhibition of v-Mos kinase by another protein kinase. Our results indicate that PKA may inhibit v-Mos via phosphorylation at the Ser-263 present in its substrate-binding domain.

* Corresponding author. Mailing address: Department of Molecular Pathology, Box 172, The University of Texas M. D. Anderson Cancer Center, 1515 Holcombe Blvd., Houston, TX 77030. Phone: (713) 794-5536. Fax: (713) 794-5518.

† Present address: Division of Molecular Virology, Baylor College of Medicine, Houston, TX 77030.

MATERIALS AND METHODS

Cell lines and culture conditions. COS-1 cells were maintained in Dulbecco's modified Eagle's medium plus 10% fetal calf serum (FCS). NIH 3T3 cells were grown in Dulbecco's modified Eagle's medium plus 8% calf serum. The NRK-6m2 cell line, which produces P85$^{gag\text{-}mos}$ encoded by the *ts*110 mutant of Mo-MuSV (3), was grown at 33°C in McCoy's 5A medium plus 12.5% FCS. At 50% confluency, the temperature was shifted to 30°C for 24 h to increase P85$^{gag\text{-}mos}$ production. Sf9 insect cells (obtained from Invitrogen, San Diego, Calif.) were grown in modified Grace's insect cell culture medium plus 10% FCS at 28°C.

Plasmids and cell transfection. For expression in COS-1 cells, the v-*mos* gene and its mutants were expressed from the simian virus 40 late promoter by using the pJC119 vector as described previously (55). The cDNA for the α isoform of the mouse PKA catalytic subunit (PKA$_c$) cloned in MT-CEVneo (33) was obtained from Eric Olson at our institution. This expression vector contains the mouse metallothionein-1 promoter. Transfections were performed by the DEAE-dextran method as described previously (55). For the stable transfection of v-*mos* expression vectors into NIH 3T3 cells, a neomycin expression vector, pKJ1 (1), was used for cotransfection and selection in the presence of geneticin (400 μg/ml; GIBCO/BRL, Gaithersburg, Md.). In pKJ1, the neomycin gene is expressed by using the mouse phosphoglycerate kinase I promoter and polyadenylation signal.

Metabolic labeling and immunoprecipitation. For labeling with [^{35}S]methionine, COS-1 cells were incubated for 30 min in methionine-free Dulbecco's modified Eagle's medium and then for 1.5 h in methionine-free medium containing 10% dialyzed FCS and 0.2 mCi of *trans*-label (ICN, Costa Mesa, Calif.) per ml. Forskolin-treated cells were labeled in the presence of 100 μM forskolin. For ^{32}P labeling, COS-1 cells were incubated for 1 h in phosphate-free Dulbecco's modified Eagle's medium containing 10% dialyzed FCS and 2 mCi of $^{32}P_i$ per ml.

After being labeled, cells were washed with Tris-buffered saline three times and solubilized in 2 ml of extraction buffer containing phosphatase, kinase, and protease inhibitors as described previously (11, 24). Cell extracts were centrifuged for 40 min at 40,000 × *g* and 4°C to remove insoluble debris. They were then incubated with 30 μl of normal rabbit serum for 15 min, and 30 μl of protein A-Sepharose (50% suspension; Pharmacia, Piscataway, N.J.) was added for 15 min on ice. The beads were removed by microcentrifugation for 1 min at 4°C, and the supernatant fraction was incubated for 1 h with anti-Mos(37–55) or anti-Mos(260–271) antibodies and then with 50 μl of protein A-Sepharose for 20 to 30 min on ice. The immunoprecipitates were collected by microcentrifugation for

1 min at 4°C and washed with extraction buffer three times. The precipitated proteins were analyzed by sodium dodecyl sulfate-polyacrylamide gel electrophoresis (SDS-PAGE) on a 10% polyacrylamide gel.

Protein kinase assays. The in vitro protein kinase assays with the v-Mos immune complexes precipitated with anti-Mos(37–55) antibodies were carried out as described previously (32, 56). Transphosphorylation of glutathione-*S*-transferase (GST)–MEK1 (K97R) by v-Mos was carried out as described previously (42). For MEK1 assays, the protein was immunoprecipitated with a monoclonal antibody (Transduction Laboratories, Lexington, Ky.). Autophosphorylation of MEK1 and phosphorylation of kinase-inactive mitogen-activated protein kinase (K52R) were carried under the same conditions as MEK1 phosphorylation by Mos. The relative amount of v-Mos was determined by Western immunoblotting as described previously (20). In some experiments, enhanced chemiluminescence detection was carried out by using the reagents and protocol from Amersham. The specificity of Mos detection by the antipeptide antibodies was routinely determined with control peptide-blocked antibodies. The relative band intensities on the autoradiograms were determined by soft-laser densitometry.

Expression and purification of GST–v-Mos protein from *Escherichia coli*. The v-*mos* gene (1.16-kb *Xba*I-*Hin*dIII fragment) was digested with nuclease S1 to eliminate the termination codon upstream of the open reading frame and then cloned into the *Sma*I site of the bacterial expression vector pGEX-3X (Pharmacia) to yield pGEX-3X:mos. This construct encodes a glutathione-*S*-transferase (GST)–v-Mos fusion protein, which also includes two additional codons present upstream of the initiation codon of v-*mos*. The construct was transformed into *E. coli* JM109, and recombinant v-Mos protein was expressed and purified essentially as described previously (15). Briefly, 100 ml of an overnight culture was diluted 1:10 in a final volume of 1,000 ml. After incubation for 1 h, isopropyl β-D-thiogalactoside (IPTG) was added to a final concentration of 0.1 mM and the cells were incubated for a further 3 h. Bacteria were harvested by centrifugation at 2,600 × *g* for 20 min at 4°C. The pellets were then resuspended and lysed in 100 ml of STE (150 mM NaCl, 50 mM Tris-HCl [pH 7.2], 1 mM EDTA) containing 500 μg of lysozyme per ml, 0.05% Nonidet P-40, 10 μg of leupeptin per ml, 10 μg of pepstatin A per ml, and 1 mM phenylmethylsulfonyl fluoride. After 10 min on ice, $MgCl_2$ and DNase A were added to final concentrations of 2.5 mM and 50 μg/ml, respectively, and the mixture was incubated on ice for a further 30 min. The lysate was centrifuged at 17,000 × *g* for 15 min at 4°C. The supernatant was incubated with 1 ml of 50% (vol/vol) glutathione-Sepharose 4B beads (Pharmacia) for 30 min at 4°C with gentle rocking. The beads were washed four times with 10 volumes of STE containing 10 μg each of leupeptin and pepstatin A per ml and 1 mM phenylmethylsulfonyl fluoride.

Expression of recombinant p37$^{v\text{-}mos}$ in insect cells. The 1.16-kb *Xba*I-*Hin*dIII fragment encompassing the entire v-*mos* gene of the myeloproliferative sarcoma virus (57), blunt ended at the *Hin*dIII site, was cloned into *Xba*I-*Sma*I-digested baculovirus expression vector pVL-1392. The resultant plasmid, pVL-v-*mos*, and the linearized BaculoGold virus DNA (Pharmingen, San Diego, Calif.) were cotransfected into Sf9 insect cells. After 4 days, the supernatant fraction was collected and more cells were infected for amplification. After that, the plaque assay was performed to pick up a single plaque. This single plaque was suspended in 0.5 ml of insect cell medium, and the cells were infected with this medium for amplification. As a result, a high-titer stock solution ($>10^8$ PFU/ml) was obtained. To this end, freshly seeded insect cells were infected with the high-titer stock solution (9×10^6 cells per T75 flask were incubated with 2 ml of the high-titer stock solution for 1 h). Then the cells were changed to fresh medium and were ready for harvesting after 40 h.

In vitro phosphorylation of v-Mos by PKA. For in vitro PKA phosphorylation reactions, 1 to 10 μg of GST, GST–v-Mos, or immunoprecipitated recombinant baculovirus-expressed v-Mos was incubated with 10 U of the bovine heart PKA catalytic subunit (PKA_c) (Sigma Chemical Co., St. Louis, Mo.) at 30°C for 30 min in a total reaction volume of 30 μl containing 40 mM Tris-HCl (pH 7.4), 20 mM magnesium acetate, 1 μl of [γ-^{32}P]ATP (4,000 Ci/mmol; NEN), and 1 μl of 1 mM ATP. For direct analysis of ^{32}P-labeled proteins, phosphorylation reactions were terminated by adding an equal volume of 2× SDS sample buffer and samples were subsequently resolved by SDS-PAGE. Phosphorylation reactions of v-Mos protein immunoprecipitated from insect cells were carried out in a similar manner.

Synthetic peptides containing potential PKA phosphorylation sites were prepared in an automated peptide synthesizer in our synthetic antigen facility. The peptides were phosphorylated with PKA as described above for Mos phosphorylation. The phosphorylated peptides were separated from unincorporated [γ-^{32}P]ATP by ascending thin-layer chromatography on cellulose plates in phosphochromatography buffer (9).

Phosphopeptide mapping analysis. For two-dimensional (2-D) peptide mapping, ^{32}P-labeled proteins were eluted from the excised gel pieces as described previously (9, 42). The proteins were each mixed with 50 μg of bovine serum albumin, precipitated with trichloroacetic acid, and oxidized with performic acid. After digestion with L-(tosylamido-2-phenyl)ethyl chloromethyl ketone (TPCK)-treated trypsin at 37°C for 18 h, the phosphopeptides were separated on cellulose plates (0.1 mm thick; Kodak, Rochester, N.Y.) as described previously (9). In the first dimension, electrophoresis was carried out in a pH 2.1 buffer (water, 88% formic acid, acetic acid [90:2:8 by volume]) for 45 min at 1,000 V. In the second dimension, separation was carried out by ascending chromatography in a solvent containing *N*-butanol, acetic acid, water, and pyridine (75:15:60:50 by volume).

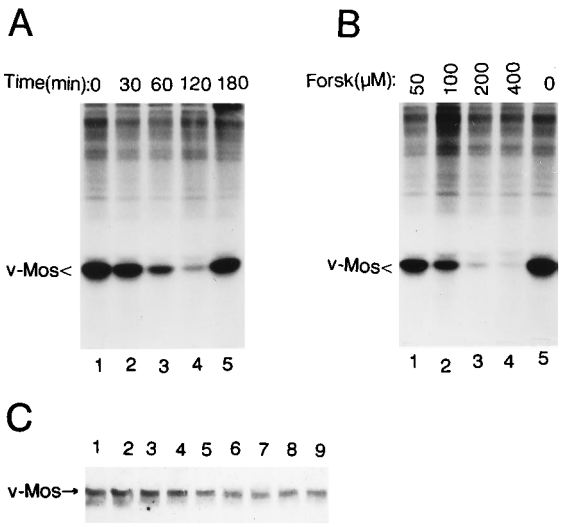

FIG. 1. Inhibition of v-Mos kinase activity by forskolin. v-*mos*-transfected COS-1 cells were treated with forskolin for different times (A) and with different dosages (B). (A and B) v-Mos was immunoprecipitated with anti-Mos(37–55) antibody and subjected to an autophosphorylation assay with [γ-^{32}P]ATP. The phosphorylated proteins were analyzed by SDS-PAGE on a 10% gel. (A) Lane 1 contains the untreated control, and lanes 2 to 5 contain cells treated with 100 mM forskolin for 30, 60, 120, and 180 min, respectively. (B) Lane 5 contains the control, and lanes 1 to 4 contain cells treated with 50, 100, 200, and 400 mM forskolin, respectively, for 90 min. (C) Cell extracts containing equal amounts of protein were subjected to Western immunoblotting with anti-Mos(37–55) antibodies. Lane 1 contains the untreated control cells; lanes 2 to 5 contain cells treated with 50, 100, 200, and 400 μM forskolin, respectively, for 90 min; and lanes 6 to 9 contain cells treated with 100 μM forskolin for 30, 60, 120, and 180 min, respectively. Exposure times were 2 h for panels A and B and 1 min (ECL procedure) for panel C.

Site-directed mutagenesis. Alanine-for-serine substitution mutants were generated by double PCR with both sense and antisense oligonucleotides containing the mutations. The template for the mutagenesis studies was the v-*mos* gene surrounded by T3 and T7 promoters in pBluescript vector (Stratagene, La Jolla, Calif.). The mutations were confirmed by DNA sequencing, and the v-*mos* gene was recloned into expression vector pJC119 or pGEX-3X.

RESULTS

Inhibition of v-Mos kinase by PKA. To examine the effect of PKA on v-Mos activity, we decided to increase the PKA activity in the cells by two different methods. First, we increased the cAMP level in cells by treatment with forskolin, a known activator of adenyl cyclase. In the second type of experiment, we overexpressed PKA_c by transfection with a plasmid DNA into COS-1 cells.

Figure 1 shows that the forskolin treatment of COS-1 cells expressing v-Mos caused a significant inhibition of v-Mos kinase that varied with the forskolin concentration and the time of treatment. The degree of v-Mos kinase inhibition increased with increases in forskolin concentration from 50 to 400 μM (Fig. 1B). Forskolin treatment did not affect the v-Mos protein level appreciably as analyzed by Western immunoblotting (Fig. 1C). The slight decrease in the v-Mos level observed at the higher forskolin concentrations (200 to 400 μM) was also insignificant compared with the nearly complete inhibition of the kinase activity (compare Fig. 1A, B, and C). Inhibition of v-Mos kinase by 100 μM forskolin increased with time up to 120 min (Fig. 1A). However, by 180 min, a good part of the inhibition was reversed. This result was reproducibly observed and may be due to attenuation or silencing of forskolin response by the cellular machinery, which operates at multiple levels (for a review, see reference 4). We also analyzed PKA

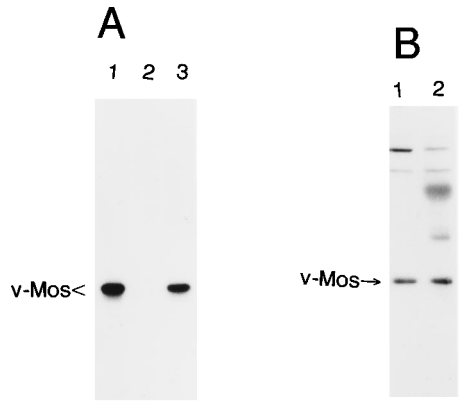

FIG. 2. Inhibition of v-Mos autokinase activity by overexpression of the PKA catalytic subunit PKA_c. (A) PKA_c and v-Mos were expressed by transient cotransfection in COS-1 cells. PKA_c- and v-Mos-encoding plasmids (5 μg each) were transfected into an 80% confluent COS-1 cells in a 100-mm-diameter dish. COS-1 cells were extracted with the lysis buffer 48 h after transfection and subjected to immune-complex kinase assay as described in Materials and Methods. v-Mos was immunoprecipitated with anti-Mos(37–55) antibody (lanes 1 and 3) or peptide-blocked antibody (lane 2) and then subjected to kinase assays. Lanes: 1 and 2, COS-1 cells transfected with the v-*mos* gene; 3: COS-1 cells cotransfected with v-*mos* and the PKA_c gene. (B) Equal amounts of total protein were subjected to Western immunoblotting with anti-Mos(37–55). Lanes: 1, v-*mos*-transfected cells; 2, PKA_c gene- and v-*mos*-cotransfected cells. Exposure times were 1.5 h for panel A and 24 h for panel B.

activity (with a Pierce colorimetric PKA assay kit, Spinzyme format) from the cells treated with forskolin. Forskolin at 100 μM caused a sharp increase in PKA activity within 30 min. It peaked at 90 min (reaching levels fivefold those of the control) and then declined, reaching close to basal level between 3 and 4 h (data not shown). The PKA activity also increased in a concentration-dependent manner in the 50 to 400 μM range. Thus, there was a good correlation between PKA activation and Mos kinase inhibition. v-Mos kinase activity was analyzed by determining autophosphorylation in immune complexes as described previously (56). Our previous studies have shown that the in vitro autophosphorylation activity of v-Mos kinase correlates with its ability to phosphorylate exogenous substrates, e.g., vimentin and MEK1 (51, 53; this study). More importantly, we have shown that v-Mos autophosphorylation sites are different from the sites of phosphorylation in vivo upon activation of PKA (see below).

v-Mos kinase activity was also inhibited upon cotransfection of the PKA_c-encoding plasmid plus a v-Mos-encoding plasmid into COS-1 cells (Fig. 2A). Western immunoblotting analysis showed that the level of the v-Mos protein remained unchanged upon coexpression of PKA_c (Fig. 2B). Furthermore, forskolin treatment or PKA_c coexpression did not affect the ability of v-Mos protein to be immunoprecipitated, as determined by [^{35}S]methionine-labeling experiments (data not shown). These results indicate that inhibition of v-Mos kinase by PKA as seen in Fig. 1 and 2 may be due to an alteration in the phosphorylation status of v-Mos. The coexpression of PKA_c by transfection into COS-1 cells resulted in a lower inhibition than the short-term forskolin treatment.

Various v-Mos proteins encoded by different isolates of Mo-MuSV expressed in different cell lines were similarly inhibited by forskolin, indicating that the inhibition is not restricted to a specific v-Mos protein or a particular cell line. Forskolin treatment inhibited another v-Mos protein, $P85^{gag\text{-}mos}$, expressed in an NRK cell line transformed by the *ts*110 mutant of Mo-MuSV (3). For $P85^{gag\text{-}mos}$, both autophosphorylation and vimentin transphosphorylation were inhibited. A similar inhibition was also observed in NIH 3T3 cells transformed by $p37^{v\text{-}mos}$ encoded by either the 124 or HT1 strain of Mo-MuSV (data not shown).

In vitro phosphorylation of v-Mos by PKA. v-Mos contains eight PKA consensus recognition sequences (four RXXS/T and four RXS/T). Therefore, we wanted to know whether PKA inhibited v-Mos kinase by directly phosphorylating the v-Mos protein. We tested this by carrying out in vitro phosphorylation reactions with purified PKA_c (Sigma Chemical Co) and two different versions of the kinase-inactive v-Mos protein. These included purified GST–v-Mos fusion protein (GST-Mos) produced in *E. coli* and $p37^{v\text{-}mos}$ produced in Sf9 insect cells with the baculovirus expression vector pVL-1392. Both proteins lacked protein kinase activity when assayed in vitro for autophosphorylation (62) or vimentin transphosphorylation activity (data not shown). This is presumably due to the lack of appropriate phosphorylation modifications. Thus, we were able to study phosphorylation of v-Mos by PKA in the absence of v-Mos autokinase activity. GST-Mos protein affinity purified by binding to GST-Sepharose was specifically phosphorylated by purified PKA_c (Fig. 3A, lane 2). As a control, purified GST protein was not phosphorylated (lane 3), indicating that the phosphorylation is restricted to the Mos domain within the GST-Mos fusion protein.

$p37^{v\text{-}mos}$ encoded by the v-*mos* gene was produced in Sf9 insect cells in relatively large amounts. SDS-PAGE of total extracts from Sf9 cells and Coomassie blue staining revealed an easily visualized v-Mos band. However, less than 10% of $p37^{v\text{-}mos}$ was in soluble form (62). $p37^{v\text{-}mos}$ immunoprecipitated from these extracts could also be phosphorylated by exogenously added PKA_c (Fig. 3B). The identity of the $p37^{v\text{-}mos}$ band in Fig. 3B, lane 3, is based on its specific

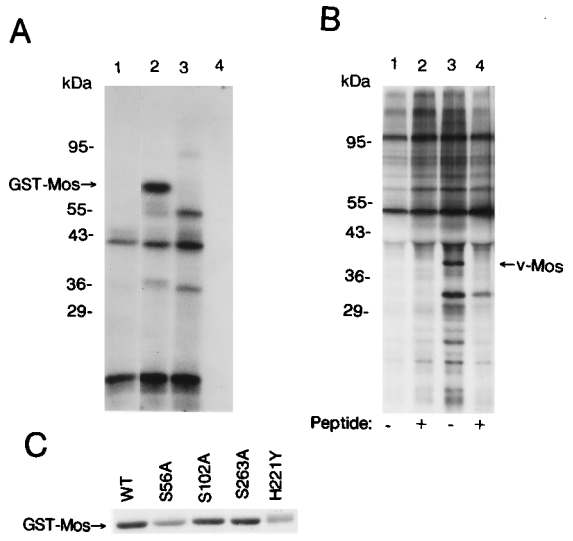

FIG. 3. In vitro phosphorylation of GST–v-Mos and $p37^{v\text{-}mos}$ by PKA. GST-Mos protein purified from bacteria and recombinant v-Mos protein immunoprecipitated from insect cells were incubated with purified PKA at 30°C for 30 min in the presence of [γ-^{32}P]ATP. (A) Lanes: 1, PKA_c alone; 2, PKA_c and 0.2 μg of GST-Mos; 3, PKA_c and GST; 4, GST-Mos alone. (B) Lanes: 1 and 2, control uninfected Sf9 cells; lanes 3 and 4, Sf9 cells infected with the v-Mos-producing recombinant baculovirus. The immunoprecipitates prepared with the unblocked (lanes 1 and 3) and peptide-blocked (lanes 2 and 4) anti-Mos(260–271) antibodies were used. (C) In vitro phosphorylation of GST-Mos containing various site-directed mutations in Mos was carried out as for the experiment in panel A. In this experiment, the S56A and H221Y mutants were present at 0.3 and 0.15 μg, respectively. All other GST-Mos proteins were present at 0.2 μg. Exposure times were 2 h for panel A, 24 h for panel B, and 1 h for panel C.

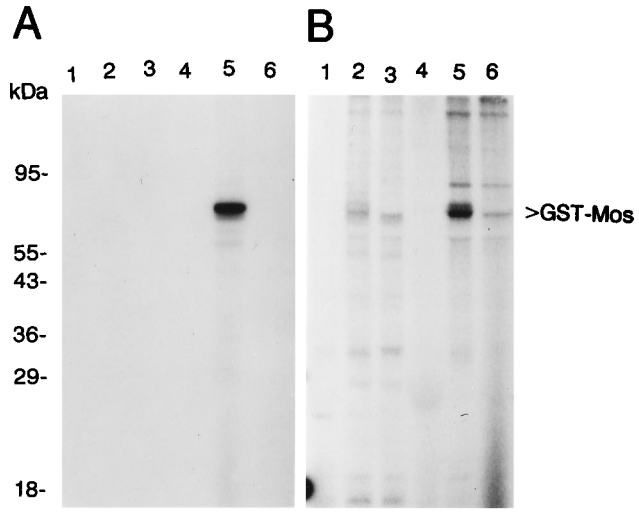

FIG. 4. Inhibition of GST-Mos kinase by PKA in vitro. (A) Activation of GST-Mos kinase by incubation in rabbit reticulocyte lysate. GST (lanes 1 and 4), GST-Mos (lanes 2 and 5), and kinase-inactive H221Y GST-Mos mutant (lanes 3 and 6) were subjected to an in vitro autophosphorylation reaction. For lanes 4 to 6, the recombinant proteins bound to glutathione beads were incubated with rabbit reticulocyte lysate (Promega, Madison, Wis.) for 30 min at 30°C and washed thoroughly five times with 20 mM *N*-2-hydroxyethylpiperazine-*N'*-2-ethanesulfonic acid (HEPES; pH 7.2)–150 mM NaCl–2 mM dithiothreitol–100 KIU of Trasylol per ml–1 mM sodium PP_i. For lanes 1 to 3, the kinase reaction was performed with no prior incubation with the reticulocyte lysate. (B) Inhibition by PKA. After incubation with rabbit reticulocyte lysate and washing, the beads containing GST (lanes 1 and 4), GST-Mos (lanes 2 and 5), and GST-Mos H221Y mutant (lanes 3 and 6) were subjected to the kinase phosphorylation reaction in the presence (lanes 1 to 3) or absence (lanes 4 to 6) of PKA_c. Exposure times were 4 h for panel A and 2 h for panel B.

recognition by anti-Mos antibody and its absence in control Sf9 insect cells. We found that the recombinant $p37^{v\text{-}mos}$ immunoprecipitated from insect cells lacked autophosphorylation activity (62). Furthermore, to totally eliminate the possibility of autophosphorylation in this experiment, immunoprecipitates were prepared with the kinase inhibitory antibody, anti-Mos(260–271) (52, 63).

Inactivation of v-Mos kinase by PKA in vitro. It was not possible to determine the functional effect of in vitro PKA phosphorylation of the recombinant Mos protein, since the Mos protein was inactive to begin with. However, upon incubation with rabbit reticulocyte lysate, GST-Mos acquired the ability to autophosphorylate (Fig. 4A). The recombinant *Xenopus* c-Mos protein fused to the maltose-binding protein is known to be activated in a similar fashion (38). Importantly, the Mos autokinase activity was inhibited upon coincubation of GST-Mos and PKA_c (compare lanes 2 and 5 in Fig. 4B). PKA phosphorylation and autophosphorylation occurred in the same reaction. Therefore, to obtain an estimate of GST-Mos phosphorylation by PKA_c, GST fused to the kinase-inactive H221Y mutant of v-Mos (58) was used as a control (Fig. 4B, lane 3). The kinase reaction shown in Fig. 4B was carried out in the presence of Mg^{2+} rather than Mn^{2+}, which would favor Mos phosphorylation by PKA at the expense of Mos autophosphorylation, which is reduced to about 50% (51). This could explain the difference between the GST-Mos autophosphorylation results seen in Fig. 4A and B. Overall, GST-Mos phosphorylation in the presence of PKA was lowered to approximately the GST-Mos (H221Y) level (compare lanes 2 and 3 in Fig. 4B). Significantly, the more slowly migrating species of GST-Mos, which typically result from v-Mos autophosphorylation (26, 32), were present in dramatically reduced amounts upon PKA_c coincubation. In this experiment, contaminating reticulocyte lysate kinase(s) also caused some phosphorylation of GST-Mos (e.g., Fig. 4B, lane 6). Overall, these results strongly suggest that PKA caused nearly complete inhibition of v-Mos kinase in vitro, similar to the inhibition of v-Mos observed in vivo upon forskolin treatment.

Identification of the phosphorylation sites on $p37^{v\text{-}mos}$. To understand the mechanism of inhibition of v-Mos kinase by PKA, the phosphorylation sites were identified by tryptic phosphopeptide mapping and by site-directed mutagenesis. Initially, we compared the 2-D tryptic phosphopeptide maps of $p37^{v\text{-}mos}$ phosphorylated in COS-1 cells in the absence and presence of coexpression of PKA_c and $p37^{v\text{-}mos}$ phosphorylated in vitro by PKA_c (Fig. 5B to D). It is evident that most of the in vivo phosphorylation of $p37^{v\text{-}mos}$ was restricted to one phosphopeptide, marked no. 1. Phosphorylation on this peptide, as well as on some additional peptides (including peptides 2 and 3), increased upon coexpression of PKA_c. Furthermore, trypsin digestion of in vitro-phosphorylated $p37^{v\text{-}mos}$ also generated peptides 2 and 3. This result was confirmed by the observed comigration of the phosphopeptides 2 and 3 generated from the in vivo- and in vitro-labeled $p37^{v\text{-}mos}$. The minor phosphopeptide 4 resulted from in vitro phosphorylation of v-Mos by PKA. However, the PKA site included in this phosphopeptide, Ser-47, is not in the optimal sequence context for PKA, nor did its phosphorylation increase in vivo upon PKA_c coexpression or forskolin treatment (compare Fig. 5B, C, and E). In fact, we have shown previously that Ser-47 may be phosphorylated in vivo by Cdc2 (6).

Serine 56 is the major PKA phosphorylation site on $p37^{v\text{-}mos}$. Initially, we used v-Mos synthetic peptides phosphorylated in vitro by PKA_c to determine the phosphorylation sites on $p37^{v\text{-}mos}$. The PKA consensus phosphorylation sequence includes an R at positions −2 and/or −3 with reference to the phosphorylatable residues S or T. The substrate recognition is enhanced if an amino acid with a hydrophobic side chain is also present at the +1 position (reviewed in reference 59). Peptides containing all eight PKA consensus phosphorylation sequences (RXXS/T or RXS/T) were synthesized (Table 1). The peptides were phosphorylated by PKA_c in vitro in the presence of [γ-^{32}P]ATP. The labeled peptides were separated from [γ-^{32}P]ATP by thin-layer chromatography on cellulose plates. The v-Mos peptides 51 to 63, 97 to 110, and 322 to 339 were phosphorylated efficiently, whereas peptides 37 to 55, 258 to 280, 354 to 364, and 363 to 374 were phosphorylated poorly. The v-Mos peptide 129 to 135 was not phosphorylated by the PKA in vitro. The v-Mos synthetic peptide, 254 to 269, in which Ser-263 was exactly in the middle, was phosphorylated as poorly as the peptide 258 to 280 (Table 1). This result indicates that the length of peptide sequences surrounding the phosphorylatable residues was adequate for in vitro phosphorylation by PKA.

The predicted 2D tryptic map positions of all seven potential PKA phosphorylation sites on $p37^{v\text{-}mos}$ are shown in Fig. 5A. This theoretical map was generated as described previously (9) and proved to be very useful as it provided the basis for further 2D mapping experiments involving comigration of trypsin-digested, in vitro-phosphorylated ^{32}P-labeled phosphopeptides and trypsin-digested [^{32}P]$p37^{v\text{-}mos}$. The phosphopeptides were digested with trypsin and subjected to a 2-D chromatography run. Some of them were mixed with trypsin digests of in vitro PKA_c-phosphorylated $p37^{v\text{-}mos}$ and then analyzed by 2D mapping (9). This type of analysis indicated that the major tryptic peptide, no. 1, is composed of v-Mos residues 54 to 63 in the sequence SCSIPLVAPR. The underlined S residue in this sequence is the phosphorylated serine 56, which is surrounded by

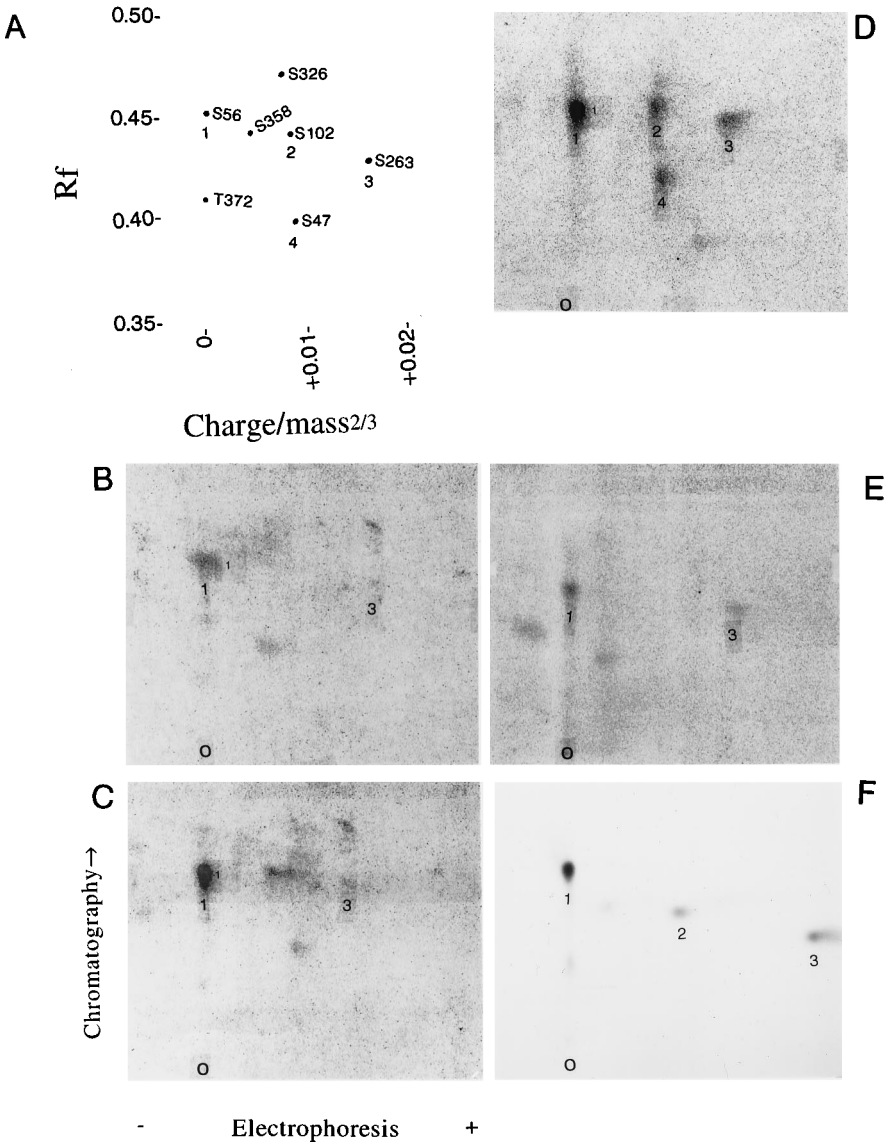

FIG. 5. 2-D phosphopeptide mapping of v-Mos. [^{32}P]v-Mos was subjected to phosphopeptide mapping as described in Materials and Methods. (A) The relative predicted positions of tryptic phosphopeptides containing various PKA phosphorylation sites were determined as described previously (9). The predictions are based on only one phosphate per peptide. The phosphopeptides are identified by the v-Mos residues that are potential PKA phosphorylation sites and by their ability to be phosphorylated by PKA in vitro. (B) v-Mos phosphorylated in vivo in COS-1 cells (342 cpm of digested sample). (C) v-Mos from COS-1 cells cotransfected with the PKA_c gene (300 cpm of digested sample). (D) Immunoprecipitated v-Mos from Sf9 cells that was phosphorylated with PKA in vitro (500 cpm of digested sample). (E) v-Mos from forskolin-treated, transfected COS-1 cells. (F) Mixture of v-Mos from forskolin-treated cells (128 cpm) and v-Mos(258–280) synthetic peptide phosphorylated with PKA_c in vitro (40 cpm). v-Mos in panels E and F is from two separate experiments. Peptide 2 is not visible in panel E but was seen at a longer exposure. Maps in panels B to E were developed on a phosphorimager, and the map in panel F was developed on an X-ray film. o, origin.

the optimal sequence for PKA recognition. The experimentally observed position of this peptide also agrees with its position predicted by the amino acid composition and charge (Fig. 5A). Figure 5E shows comigration of tryptic peptides containing Ser-263 phosphorylated in v-Mos in forskolin-treated cells and the synthetic peptide phosphorylated by PKA_c in vitro.

Coexpression of PKA_c in COS-1 cells resulted in increased phosphorylation at v-Mos residues Ser-56, Ser-102, and Ser-263, indicated as phosphopeptides 1, 2, and 3, respectively (Fig. 5C). However, forskolin treatment, which resulted in the maximum (although transient) inhibition (Fig. 1), correlated with increased in vivo phosphorylation at Ser-263 (Fig. 5E). Comparison of relative intensities of the spots representing different phosphopeptides suggested that phosphorylation at Ser-263 may be responsible for v-Mos inhibition by PKA. On the basis of the peptide-mapping studies alone, the inhibitory role of Ser-56 phosphorylation could not be ruled out, since Ser-56 was phosphorylated under all conditions (Fig. 5).

In vitro mutagenesis studies. To confirm the identity of the potential phosphorylation sites and determine their functional significance, serine residues 56, 102, and 263 were substituted by alanine. Ser-56 lies outside the kinase domain. Ser-102 lies near the conserved glycine-rich sequence present in protein kinases that is important for ATP binding (23). Ser-263 lies between protein kinase subdomains VII and VIII, a region important for substrate recognition by the catalytic domain

TABLE 1. Phosphorylation of v-Mos synthetic peptides by PKA_c

Residue no.	Sequence[a]	Relative phosphorylation
37–55	SLCRYLPRELSPSVDSRSC	+
51–63	DSRSCSIPLVAPR	++++
97–110	MHRLGSGGFGSVYK	++
129–135	DLRASQR	–
254–269	LQVLRGRQASPPHIGG	+
258–280	RGRQASPPHIGGTYTHQAPEILK	+
322–339	NLRPSLAGAVFTASLTGK	++++
354–364	LQRPSAELLQR	+
363–374	QRDLKAFRGTLG	+

[a] The potential PKA phosphorylation sites and the upstream recognition sequences are underlined. The sequences are from reference 61. In vitro phosphorylation of v-Mos synthetic peptides by PKA_c was carried out as described in Materials and Methods.

(23). As described above, Ser-56 appears to be the major phosphorylation site. Ser-263 phosphorylation correlates with forskolin treatment, and Ser-102 is phosphorylated by PKA in vitro and upon forskolin treatment or coexpression of PKA_c in vivo.

v-Mos and its mutants containing alanine at positions 56, 102, and 263 (indicated as S56A, S102A, and S263A, respectively, in Fig. 6 to 8) were expressed in COS-1 cells. The [^{35}S]methionine- or $^{32}P_i$-labeled v-Mos protein was immunoprecipitated from cell lysates and analyzed by SDS-PAGE (Fig. 6). As described previously (32, 40), [^{35}S]methionine-labeled v-Mos protein migrated as two species. The more slowly migrating species corresponds to the hyperphosphorylated form (40). The S56A mutant of v-Mos migrated as a single band and corresponds to the faster-migrating species. The other two v-Mos mutants, S102A and S263A, migrated like wild-type v-Mos (Fig. 6A). The ^{32}P in vivo-labeling experiment showed that phosphorylation of the S56A mutant, but not the other two mutants, was dramatically reduced when compared with that of wild-type v-Mos (Fig. 6B). Thus, our results strongly suggest that Ser-56 is the major in vivo phosphorylation site on v-Mos. Comparison of the intensities of two [^{35}S]methionine-labeled v-Mos bands suggests that approximately 25% of v-Mos molecules are phosphorylated at Ser-56.

Forskolin treatment did not affect the mobility of v-Mos or any of the mutants (Fig. 6A). This is consistent with the interpretation derived from the peptide-mapping data that the forskolin treatment did not significantly increase the phosphorylation at Ser-56. The mutagenesis studies suggested that the phosphorylation at Ser-102 or Ser-263 may not result in altered mobility during SDS-PAGE. However, since only a small percentage of v-Mos is phosphorylated at these residues, this issue remains unresolved.

Various site-directed v-Mos mutants were also expressed as GST-Mos and purified from *E. coli*. All these were phosphorylated by PKA_c in vitro (Fig. 3C), and analysis of their tryptic peptide maps further supported our assignment of phosphorylation sites at Ser-56, Ser-102, and Ser-263. The spots 1, 2, and 3 were found missing in tryptic maps of S56A, S102A and S263A mutants respectively.

The significance of phosphorylation at the major phosphorylation site, Ser-56, was examined by determining the kinase activity of the S56A mutant in an in vitro autophosphorylation reaction. The results of one such experiment with stably transfected NIH 3T3 cells are shown in Fig. 7A. The S56A mutant showed autokinase activity comparable to that of the wild-type v-Mos. Similar results were obtained upon transient expression of the S56A mutant in COS-1 cells (data not shown). As determined by Western immunoblotting, levels of the mutant and wild-type v-Mos protein were the same (62). In some experi-

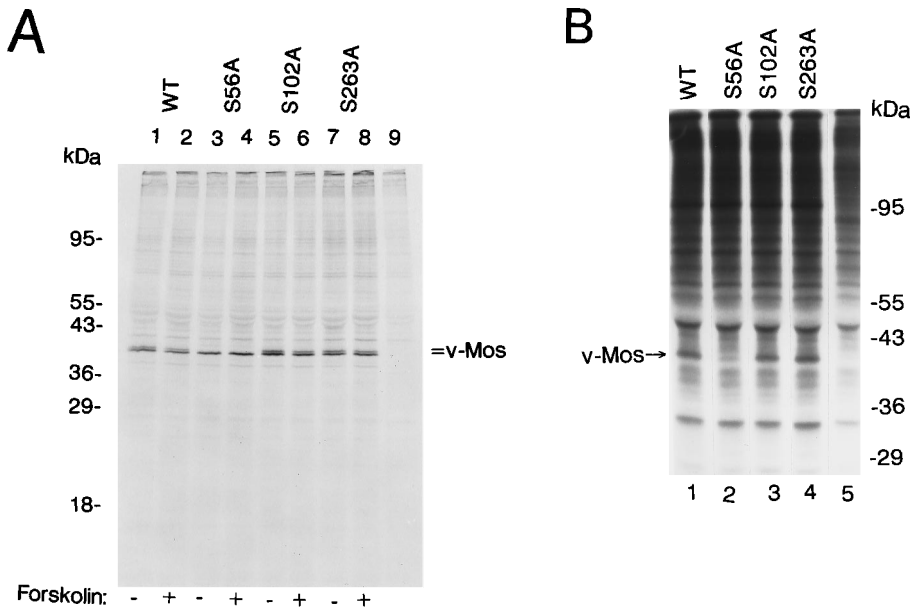

FIG. 6. Effect of phosphorylation site mutations on the in vivo labeling of v-Mos. (A) The alanine 56 mutant of v-Mos does not yield the form that migrates more slowly in SDS-PAGE. v-Mos (lanes 1 and 2) and its various alanine-for-serine mutants were immunoprecipitated with the anti-Mos(37–55) antibodies from the transfected COS-1 cells after being labeled with [^{35}S]methionine for 90 min. Where indicated, 200 mM forskolin was added to the cells along with [^{35}S]methionine. Lane 9 shows control immunoprecipitate from the v-*mos*-transfected cells prepared with the peptide-blocked antibody. (B) Normal and mutant versions of v-Mos were labeled with $^{32}P_i$ in the transfected COS-1 cells, and anti-Mos(37–55) immunoprecipitates were analyzed by SDS-PAGE. Lane 5 shows control immunoprecipitate from the v-*mos*-transfected cells prepared with the peptide-blocked antibody. Molecular mass markers are shown on the sides. Exposure times were 48 h for panel A and 10 h for panel B.

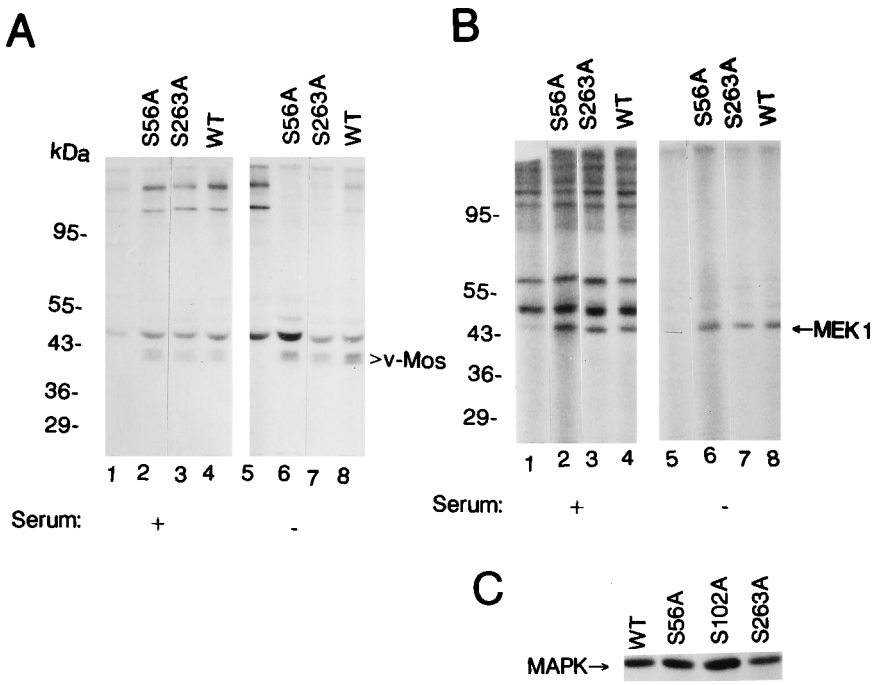

FIG. 7. Lack of effect of the S56A mutation on v-Mos in vitro kinase activity and in vivo MEK1 activation in stably transformed NIH 3T3 cells. In vitro v-Mos (A) or MEK1 (B) autophosphorylation assays were carried out with normally growing cells (lanes 1 to 4) or cells starved for serum for 24 h (lanes 5 to 8). Lanes 1 and 5 in each panel contain normally growing and serum-starved nontransfected NIH 3T3 cells, respectively. (C) Phosphorylation of mitogen-activated protein (MAPK) kinase by MEK1. In an experiment similar to the one shown in panel B, MEK1 immunoprecipitates from serum-starved cells were used to phosphorylate kinase-inactive mitogen-activated protein kinase (K52R). In this experiment, somewhat reduced MEK1 activity in S263A v-Mos-transformed cells is due to the presence of proportionally less v-Mos protein. Exposure times were 6 h for panel A, 2 h for panel B, and 1 h for panel C.

ments, we observed a 25 to 50% decrease in v-Mos autokinase activity as a result of the S56A mutation. These results suggest that the phosphorylation at Ser-56 may have a stimulatory rather than inhibitory effect. However, they also suggest that Ser-56 phosphorylation is not essential for the protein kinase activity of $p37^{v\text{-}mos}$.

The key substrate of v-Mos kinase in transformed cells is the mitogen-activated protein kinase/ERK kinase MEK (30, 36, 38, 42, 43, 50). Therefore, we examined whether Ser-56 phosphorylation is necessary for MEK1 activation in stably transfected NIH 3T3 cells, which are often used for cellular transformation assays. MEK1 was immunoprecipitated from normally growing cells or after serum starvation for 24 h and subjected to autophosphorylation reaction (Fig. 7B). In vitro autophosphorylation of the activated MEK1 correlates with its ability to phosphorylate mitogen-activated protein kinase (36, 42, 44). The experimental results shown in Fig. 7B and C demonstrate that the ability of v-Mos to activate MEK1 was not affected by the S56A mutation.

Under conditions of normal growth, when an increase in the PKA activity was not forced, the S263A mutation also did not affect v-Mos kinase activity and its ability to activate MEK1 (Fig. 7B and C). Finally, we tested the ability of the alanine-for-serine substitutions to abrogate the forskolin-mediated inhibition of v-Mos kinase. The inhibitory effect of forskolin on v-Mos kinase was abrogated by the S263A mutation but not by the S56A or S102A mutation (Fig. 8A). In this experiment, the magnitude of v-Mos kinase inhibition was somewhat smaller than the inhibition seen in the experiment illustrated in Fig. 1. Nevertheless, this result is consistent with all the data presented above and strongly suggests that PKA inhibits v-Mos kinase via phosphorylation at Ser-263. Similar results were

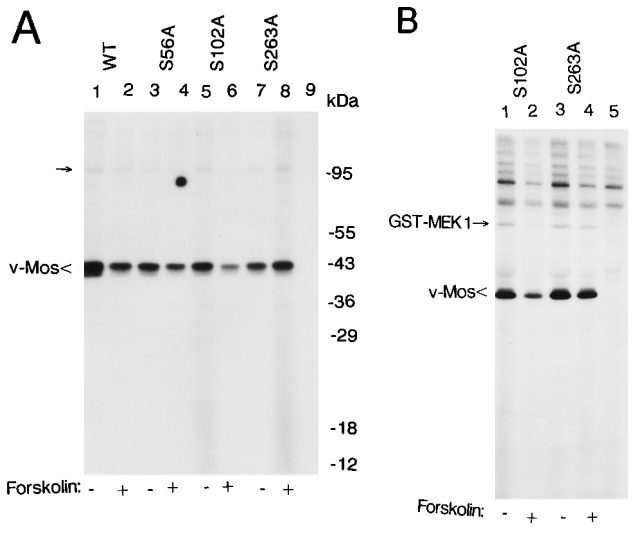

FIG. 8. Lack of forskolin effect on S263A v-Mos activity. (A) v-Mos and its phosphorylation site mutants were produced in COS-1 cells by transient transfection, and v-Mos immunoprecipitates were subjected to an autophosphorylation assay. Where indicated, the cells were treated with 100 mM forskolin for 90 min before being harvested for kinase assay. In this experiment, the level of wild-type (WT) Mos protein, as determined by Western immunoblotting, was approximately 1.5 times that of the mutants. Lane 9 contains the control in which the peptide-blocked antibody was used for immunoprecipitation. (B) Transphosphorylation of GST-MEK (K97R). The experiment was carried out as for panel A, except that 1 μg kinase-inactive GST-MEK1 was included in the reaction. Total products were analyzed by SDS-PAGE. Lane 5 contains the control in which the peptide-blocked antibody was used for immunoprecipitation. The 105-kDa protein indicated by an arrow in panel A coprecipitated with v-Mos. Exposure times were 1 h for panel A and 30 min for panel B.

obtained when S263A mutant of v-Mos was assayed for its ability to phosphorylate GST-MEK1 (Fig. 8B). Even though it is possible that forskolin treatment causes phosphorylation at additional sites, including Ser-102 (Fig. 5F), this experiment suggests that phosphorylation at Ser-263 is responsible for forskolin inhibition of v-Mos kinase.

Autophosphorylation pattern of v-Mos and its mutants. In this study, we used mostly in vitro autophosphorylation as a measure of v-Mos activity, because it is the most sensitive assay and it correlates well with the transphosphorylation activity on an exogenously added substrate, e.g., vimentin (51, 53). However, interpretation of the data would be difficult if autophosphorylation sites were also the PKA phosphorylation sites. To address this concern, tryptic phosphopeptide maps of in vitro-autophosphorylated v-Mos and its mutants, S56A and S263A, were compared. All three maps are identical, ruling out the possibility that Ser-56 and Ser-263 are autophosphorylation sites (data not shown). Furthermore, examination of tryptic maps of in vivo-phosphorylated v-Mos under various conditions showed no evidence of increased phosphorylation at sites that are autophosphorylated in vitro.

Only a small fraction of p37$^{v\text{-}mos}$ is active as protein kinase. We wanted to determine what fraction of v-Mos protein was active in our in vitro protein kinase assays, since this information may be important in understanding the role of phosphorylation in the regulation of v-Mos kinase activity. Two identical flasks of NIH 3T3 cells were infected with Mo-MuSV. After 40 h, one flask was labeled with [^{35}S]methionine for 2 h. Immune complexes prepared from both flasks were then subjected to an autophosphorylation assay with [γ-^{32}P]ATP in the case of the nonlabeled flask and nonradioactive ATP in the case of the [^{35}S]methionine-labeled flask. Within 10 min of the kinase reaction, all the ^{32}P-labeled p37$^{v\text{-}mos}$ migrated to a band usually occupied by the hyperphosphorylated species termed p43$^{v\text{-}mos}$. However, in a parallel reaction, essentially all of ^{35}S-labeled p37$^{v\text{-}mos}$ migrated to the initial position characteristic of its hypophosphorylated form (data not shown). Considering the sensitivity of detection in this type of experiment, we believe that more than 90% of ^{35}S-labeled p37$^{v\text{-}mos}$ stayed in the hypophosphorylated form after the kinase reaction and was therefore inactive. In a similar experiment, we previously found that most of the v-Mos produced by in vitro translation in rabbit reticulocyte lysate was also inactive (26). Whether a large percentage of v-Mos is also inactive in vivo is a more difficult question. Thinking about it another way, the percentage of v-Mos protein that must be phosphorylated by PKA to achieve the inhibition of v-Mos kinase seen in our experiments is very small. Thus, the phosphorylation sites that are important for inhibition need not be seen as major phosphopeptides in our tryptic peptide analysis. In other words, if the inhibitory phosphorylation at Ser-263 is preferentially directed to the active v-Mos population, one might achieve a nearly complete inhibition of the v-Mos kinase, as observed in the experiments shown above (Fig. 1).

DISCUSSION

Identification of the major v-Mos phosphorylation site. We have identified Ser-56 as the major in vivo phosphorylation site in v-Mos. This highlights a significant difference between the in vivo phosphorylation patterns of c-Mos^{xe} and v-Mos. Freeman et al. (19) found that in c-Mos^{xe}, Ser-3, the equivalent of Ser-34 in v-Mos, is the major in vivo phosphorylation site. Studies by Nishizawa et al. (37) further showed that the autophosphorylation at Ser-3 is essential for the stability of c-Mos in the egg. Phosphorylation at Ser-3 is also important for the Mos interaction with MEK1 (12). Our results presented here indicate that Ser-34 is not a major in vivo phosphorylation site on v-Mos even though it may be autophosphorylated in vitro (5). Our results also indicate that Ser-56, which is the major phosphorylation site on v-Mos, is not phosphorylated by the autokinase reaction. So far, we have been unable to map phosphorylation sites on c-Mos because of low ^{32}P incorporation and the presence of other comigrating proteins during SDS-PAGE.

Although Ser-56 is evolutionarily conserved in c-Mos (45), its substitution by alanine did not affect the ability of v-Mos to autophosphorylate in vitro or activate MEK1 in vivo. Similarly, Ser-102, which may be a minor in vivo phosphorylation site, does not appear to be important for v-Mos enzyme activity. These results agree with those of a study by Freeman et al. (19) in which alanine-for-serine substitutions at positions corresponding to the v-Mos Ser-56 and Ser-102 in *Xenopus* c-Mos did not affect its ability to either induce oocyte maturation or function as the cytostatic factor.

Mechanism of PKA inhibition. In this study, we have shown that an increase in PKA activity results in the inhibition of v-Mos kinase activity in vivo. The inhibition was observed upon the activation of adenylate cyclase as a result of forskolin addition or upon overexpression of PKA$_c$. Another activator of PKA, 8-bromo-cAMP, also inhibited v-Mos activity (data not shown). In our experiments, the inhibition manifested as a decrease in the extent of v-Mos autophosphorylation. The rate of phosphorylation is linear for only part of the duration of reaction (32). Therefore, the rate of enzyme reaction (measured as the rate of phosphorylation in the early linear period of reaction) is most probably more inhibited than is apparent in Fig. 1 and 2. The protein kinase activities of all the v-Mos proteins tested in these studies, e.g., P85$^{gag\text{-}mos}$ and p37$^{v\text{-}mos}$ encoded by 124 and HT1 strains of Mo-MuSV, were inhibited by PKA (Fig. 1 and 2 and data not shown). Inhibition of p37$^{v\text{-}mos}$-HT1 may be significant because its sequence from residues 32 to 374 is identical to that of c-Mos (49). Furthermore, the truncated v-Mos protein produced by the translational initiation at the second AUG, which is similar to c-Mos in structure and enzyme activity, was also inhibited by PKA to a similar degree to that of full-length v-Mos (62).

In support of our results regarding v-Mos inhibition by PKA, both Mos and PKA are known to localize to microtubules, the latter through its regulatory subunit (reviewed in reference 34). Most significantly, we have identified the phosphorylation site responsible for the inhibition of v-Mos kinase by direct phosphorylation by PKA. In the present study, the phosphorylation at this site, Ser-263, increased significantly upon forskolin treatment. However, the site may still be phosphorylated only in a small percentage of v-Mos molecules. To explain this result, we propose that inhibitory phosphorylation may be specifically directed to the active population of v-Mos molecules.

Forskolin-induced inhibition of v-Mos is seen only upon short-term treatment. The lack of forskolin effect at later times may be due to attenuation or silencing of PKA activity, both of which are known to occur (4). This would also explain why PKA$_c$ coexpression yields lower inhibition of v-Mos than forskolin treatment (compare Fig. 1 and 2). The attenuation and silencing of the effects of PKA are achieved through a reduction in the level of its catalytic subunit and through dephosphorylation of PKA substrates by the increased phosphatase activity, which may colocalize with PKA through binding to a common anchoring protein (for reviews, see references 13 and 34). Of course, the differences in the subcellular localization of active PKA molecules that phosphorylate Mos under different experimental conditions may also contribute to the differences

in the degree of inhibition. There is some evidence that PKA must compartmentalize with its substrates in order to function. The PKA-mediated inhibition of v-Mos may also be influenced by v-Mos phosphorylation at other sites. For example, in our study, the S263A mutant of v-Mos not only lacked the ability to be inhibited by forskolin treatment but also was modestly stimulated under these conditions (Fig. 8). The inhibitory and stimulatory phosphorylations on v-Mos may be carried out by different isoforms of PKA in vivo. If this is true, the inhibitory and stimulatory phosphorylations being carried out by different isoforms of the same protein kinase would not be unique for Mos. As an example, the transcription factor cAMP-responsive element-binding protein (CREB) is phosphorylated by CaM kinase II at both Ser-133 and Ser-142. Ser-133 phosphosphorylation stimulates the CREB activity, while Ser-142 phosphorylation inhibits it (reviewed in reference 21). Interestingly, the CaM kinase IV phosphorylates only Ser-133 but not Ser-142. In the case of Mos, resolution of these issues will require further studies into the regulation of its kinase activity.

Surprisingly, the S263A mutation caused no increase in the v-Mos kinase activity in transfected cells. This result can be explained if one considers that the inhibitory effect of Ser-263 phosphorylation is completely reversed by another event such as a specific phosphorylation or dephosphorylation at another residue. The short-term forskolin treatment may tip the balance toward inhibition due to increased phosphorylation at Ser-263. Our result with the S263A v-Mos mutant is consistent with the observation by Freeman and Donoghue (17) that this mutation does not affect the focus-forming ability of v-Mos. However, as Freeman and Donoghue (17) also observed, the S358A mutation reduced the focus-forming ability of v-Mos to 58% of the control value, and the double mutant of v-Mos containing the S358A and S263A mutations had somewhat increased transforming activity (73% of the control value). Together, these results suggest that under certain conditions, the S263A mutation could cause an increase in v-Mos transforming activity.

The role of PKA phosphorylation at various sites other than Ser-263 remains to be understood. Of interest, the alanine-for-serine substitution at residue 326, which is phosphorylated strongly by PKA in a v-Mos synthetic peptide (Table 1), caused a dramatic reduction in v-Mos autokinase activity and transforming activity (17). In that study, the S358A mutation also had an inhibitory effect, which synergized with the inhibition by the S326A mutation (17). Further work is also needed to conclusively determine whether that Ser-263 is indeed phosphorylated by PKA or other protein kinases in vivo. It is well known that PKA interdigitates with various signaling pathways at multiple points (10, 22, 27, 31, 35). Thus, it is possible that the differences in the effect of forskolin treatment for various times and also between forskolin treatment and PKA_c coexpression are due to differences in the activation status of some of these pathways.

Vande Woude and colleagues have examined the mechanism of PKA inhibition of Mos-induced oocyte maturation in *X. laevis* (16, 31). According to their studies, PKA does not influence Mos activity directly. Discrepancy between their data and ours may be due to species difference (*Xenopus* c-Mos versus v-Mos protein, which is similar to mouse c-Mos). In support of this interpretation, we note that Ser-263 is absent in *Xenopus* c-Mos (45). Threonine at position 228 in *Xenopus* Mos, which is equivalent to residue 262 in v-Mos, is not a PKA consensus site. Inhibition by posttranslational regulation of Mos kinase activity may be more important in mice than in frogs (24, 63, 64). Initiation of meiosis I requires new synthesis of Mos in *Xenopus* oocytes, but meiosis I can be completed in mouse oocytes without new synthesis of Mos (39), presumably because of activation of already existing low levels of Mos protein (41, 63, 64). We propose that Mos kinase is kept inactive in fully grown mouse oocytes by PKA. We believe that the prophase-arrested immature oocytes, with unusually high levels of PKA activity, may be more comparable to forskolin-treated cells.

ACKNOWLEDGMENTS

This study was supported by National Institutes of Health grants CA 45125 and CA 16672. R.B.A. holds the Hubert L. Stringer Chair in Cancer Research.

We thank Steve Maxwell, Department of Thoracic Surgery, for advice on the baculovirus expression system and Francis Pham for help with some experiments. We also thank Sandra Classen and Tammy Trlicek for manuscript preparation.

REFERENCES

1. **Adra, C. N., P. H. Boer, and M. W. McBurney.** 1987. Cloning and expression of the mouse *pgk*-1 gene and the nucleotide sequence of its promoter. Gene **60:**65–74.
2. **Al-Bagdadi, F., B. Singh, and R. B. Arlinghaus.** 1990. Evidence for involvement of the protein kinase C pathway in the activation of $p37^{v\text{-}mos}$ protein kinase. Oncogene **5:**1251–1257.
3. **Arlinghaus, R. B.** 1985. The ts110 Moloney mouse sarcoma virus system: *gag-mos* gene products and cellular transformation. J. Gen. Virol. **66:**1845–1853.
4. **Armstrong, R., W. Wen, J. Meinkoth, S. Taylor, and M. Montminy.** 1995. A refractory phase in cyclic AMP-responsive transcription requires down regulation of protein kinase A. Mol. Cell. Biol. **15:**1826–1832.
5. **Bai, W., R. B. Arlinghaus, and B. Singh.** Unpublished data.
6. **Bai, W., B. Singh, W. L. Karshin, R. A. Shonk, and R. B. Arlinghaus.** 1991. Phosphorylation of v-Mos Ser-47 by the mitotic form of $p34^{cdc2}$. Oncogene **6:**1715–1723.
7. **Bai, W., B. Singh, Y. Yang, L. S. Ramagli, M. Nash, N. K. Herzog, and R. B. Arlinghaus.** 1992. The physical interaction between $p37^{env\text{-}mos}$ and tubulin structures. Oncogene **7:**493–500.
8. **Bornslaeger, E. A., P. Mattei, and R. M. Schultz.** 1986. Involvement of cAMP-dependent protein kinase and protein phosphorylation in regulation of mouse oocyte maturation. Dev. Biol. **114:**453–462.
9. **Boyle, W. J., P. van der Geer, and T. Hunter.** 1991. Phosphopeptide mapping and phosphoamino acid analysis by two-dimensional separation on thin-layer cellulose plates. Methods Enzymol. **201:**110–149.
10. **Burgering, B. M., G. J. Pronk, P. C. vanWeeren, P. Chardin, and J. L. Bos.** 1993. cAMP antagonizes $p21^{ras}$-directed activation of extracellular signal-regulated kinase 2 and phosphorylation of mSos nucleotide exchange factor. EMBO J. **12:**4211–4220.
11. **Chackalaparampil, I., and D. Shalloway.** 1988. Altered phosphorylation and activation of $pp60^{c\text{-}src}$ during fibroblast mitosis. Cell **52:**801–810.
12. **Chen, M., and J. C. Cooper.** 1995. Ser-3 is important for regulating Mos interaction with and stimulation of mitogen-activated protein kinase kinase. Mol. Cell. Biol. **15:**4727–4734.
13. **Coghlan, V. M., B. A. Perrino, M. Howard, L. K. Langeberg, J. B. Hicks, W. M. Gallatin, and J. D. Scott.** 1995. Association of protein kinase A and protein phosphatase 2B with a common anchoring protein. Science **267:**108–111.
14. **Colledge, W. W., M. B. L. Carlton, G. B. Udy, and M. J. Evans.** 1994. Disruption of c-*mos* causes parthenogenetic development of unfertilized mouse eggs. Nature (London) **370:**65–68.
15. **Crews, C. M., A. A. Alessandrini, and R. L. Erikson.** 1991. Mouse Erk-1 gene product is a serine/threonine protein kinase that has the potential to phosphorylate tyrosine. Proc. Natl. Acad. Sci. USA **88:**8845–8849.
16. **Daar, I., N. Yew, and G. F. Vande Woude.** 1993. Inhibition of *mos*-induced oocyte maturation by protein kinase A. J. Cell Biol. **120:**1197–1202.
17. **Freeman, R. S., and D. J. Donoghue.** 1989. Transforming mutant v-*mos* protein kinases that are deficient in in vitro autophosphorylation. Mol. Cell. Biol. **9:**4087–4090.
18. **Freeman, R. S., J. P. Kanki, S. M. Ballantyne, K. M. Pickham, and D. J. Donoghue.** 1990. Effects of the v-*mos* oncogene on *Xenopus* development: meiotic induction in oocytes and mitotic arrest in cleaving embryos. J. Cell Biol. **111:**533–541.
19. **Freeman, R. S., A. N. Meyer, J. Li, and D. J. Donoghue.** 1992. Phosphorylation of conserved serine residues does not regulate the ability of mos^{xe} protein kinase to induce oocyte maturation or function as cytostatic factor. J. Cell Biol. **116:**725–735.
20. **Gallick, G. E., J. T. Sparrow, B. Singh, S. A. Maxwell, L. H. Stanker, and R. B. Arlinghaus.** 1985. Recognition of *mos*-related proteins with an antiserum to a peptide of the v-*mos* gene product. J. Gen. Virol. **66:**945–955.

21. **Ghosh, A., and M. E. Greenberg.** 1995. Calcium signaling in neurons: molecular mechanisms and cellular consequences. Science **268:**239–247.
22. **Hafner, S., H. S. Adler, H. Mischak, P. Janosch, G. Heidecker, A. Wolfman, S. Pippig, M. Lohse, M. Ueffing, and W. Kolch.** 1994. Mechanism of inhibition of Raf-1 by protein kinase A. Mol. Cell. Biol. **14:**6696–6703.
23. **Hanks, S. K., A. M. Quinn, and T. Hunter.** 1988. The protein kinase family: conserved features and deduced phylogeny of the catalytic domains. Science **241:**42–52.
24. **Hashimoto, N., and T. Kishimoto.** 1988. Regulation of meiotic metaphase by a cytoplasmic maturation-promoting factor during mouse oocyte maturation. Dev. Biol. **126:**242–252.
25. **Hashimoto, N., N. Watanabe, Y. Furuta, H. Tamemoto, N. Sagata, M. Yokoyama, K. Okazaki, M. Nagayoshi, N. Takeda, Y. Ikawa, and S. Aizawa.** 1994. Parthenogenetic activation of oocytes in c-*mos*-deficient mice. Nature (London) **370:**68–71.
26. **Herzog, N. K., M. Nash, L. S. Ramagli, and R. B. Arlinghaus.** 1990. v-*mos* protein produced by in vitro translation has protein kinase activity. J. Virol. **64:**3093–3096.
27. **Hunter, T.** 1995. Protein kinases and phosphatases: the yin and yang of protein phosphorylation and signaling. Cell **80:**225–236.
28. **Liu, J., B. Singh, D. Wlodek, and R. B. Arlinghaus.** 1990. Cell cycle dependent structural and functional alteration of $P85^{gag\text{-}mos}$ protein kinase activity. Oncogene **5:**171–178.
29. **Maller, J.** 1983. Interaction of steroids with the cyclic nucleotide system in amphibian oocytes. Adv. Cyclic Nucleotide Res. **15:**295–236.
30. **Mansour, S. J., W. T. Matten, A. S. Hermann, J. M. Candia, S. Rong, K. Fukasawa, G. F. Vande Woude, and N. G. Ahn.** 1994. Transformation of mammalian cells by constitutively active MAP kinase kinase. Science **265:** 966–970.
31. **Matten, W., I. Daar, and G. F. Vande Woude.** 1994. Protein kinase A acts at multiple points to inhibit *Xenopus* oocyte maturation. Mol. Cell. Biol. **14:** 4419–4426.
32. **Maxwell, S. A., and R. B. Arlinghaus.** 1985. Serine kinase activity associated with Moloney murine sarcoma virus 124-encoded $p37^{mos}$. Virology **143:** 321–333.
33. **Mellon, P. L., C. H. Clegg, L. A. Correll, and G. S. McKnight.** 1989. Regulation of transcription by cyclic AMP-dependent protein kinase. Proc. Natl. Acad. Sci. USA **86:**4887–4891.
34. **Mochly-Rosen, D.** 1995. Localization of protein kinases by anchoring proteins: a theme in signal transduction. Science **268:**247–251.
35. **Monfar, M., K. P. Lemon, T. C. Grammer, L. Cheatham, J. Chung, C. J. Vlahos, and J. Blenis.** 1995. Activation of pp70/85 S6 kinases in interleukin-2-responsive lymphoid cells is mediated by phosphatidylinositol 3-kinase and inhibited by cyclic AMP. Mol. Cell. Biol. **15:**326–337.
36. **Nebreda, A. R. and T. Hunt.** 1993. The c-*mos* proto-oncogene protein kinase turns on and maintains the activity of MAP kinase, but not MPF, in cell-free extracts of *Xenopus* oocytes and eggs. EMBO J. **12:**1979–1986.
37. **Nishizawa, M., K. Okazaki, N. Furuno, N. Watanabe, and N. Sagata.** 1992. The "second-codon rule" and autophosphorylation govern the stability and activity of Mos during the meiotic cell cycle in *Xenopus* oocytes. EMBO J. **11:** 2433–2446.
38. **Okazaki, K., and N. Sagata.** 1995. MAP kinase activation is essential for oncogenic transformation of NIH 3T3 cells by Mos. Oncogene **10:**1149–1157.
39. **O'Keefe, S. J., H. Wolfes, A. A. Kiessling, and G. M. Cooper.** 1989. Microinjection of antisense c-*mos* oligonucleotides prevents meiosis II in the maturing mouse egg. Proc. Natl. Acad. Sci. USA **86:**7038–7042.
40. **Papkoff, J., I. M. Verma, and T. Hunter.** 1982. Detection of a transforming gene product in cells transformed by Moloney murine sarcoma virus. Cell **29:** 417–426.
41. **Paules, R. S., R. Buccione, R. C. Moschel, G. F. Vande Woude, and J. J. Eppig.** 1989. Mouse *mos* proto-oncogene product is present and functions during oogenesis. Proc. Natl. Acad. Sci. USA **86:**5395–5399.
42. **Pham, C. D., R. B. Arlinghaus, C.-F. Zheng, K.-L. Guan, and B. Singh.** 1995. Characterization of MEK1 phosphorylation by the v-Mos protein. Oncogene **10:**1683–1688.
43. **Posada, J., N. Yew, N. G. Ahn, G. F. Vande Woude, and J. A. Cooper.** 1993. Mos stimulates MAP kinase in *Xenopus* oocytes and activates a MAP kinase kinase in vitro. Mol. Cell. Biol. **13:**2546–2553.
44. **Resing, K., S. J. Mansour, A. S. Hermann, R. S. Johnson, J. M. Candia, K. Fukasawa, G. F. Vande Woude, and N. G. Ahn.** 1995. Determination of v-Mos-catalyzed phosphorylation sites and autophosphorylation sites on MAP kinase kinase by ESI/MS. Biochemistry **34:**2610–2620.
45. **Sagata, N., M. Oskarsson, T. Copeland, J. Brumbaugh, and G. F. Vande Woude.** 1988. Function of c-*mos* proto-oncogene product in meiotic maturation in *Xenopus* oocytes. Nature (London) **335:**519–525.
46. **Sagata, N., N. Watanabe, G. F. Vande Woude, and Y. Ikawa.** 1989. The c-*mos* proto-oncogene product is a cytostatic factor responsible for meiotic arrest in vertebrate eggs. Nature (London) **342:**512–518.
47. **Schorderet-Slatkine, S., M. Schorderet, and E. E. Baulieu.** 1982. Cyclic AMP-mediated control of meiosis: effects of progesterone, cholera toxin, and membrane-active drugs in *Xenopus laevis* oocytes. Proc. Natl. Acad. Sci. USA **79:**850–854.
48. **Schultz, R. M., R. R. Montgomery, and J. R. Belanoff.** 1983. Regulation of mouse oocyte meiotic maturation: implication of a decrease in oocyte cAMP and protein dephosphorylation in commitment to resume meiosis. Dev. Biol. **97:**264–273.
49. **Seth, A., and G. F. Vande Woude.** 1985. Nucleotide sequence and biochemical activity of the Moloney murine sarcoma virus strain HT-1 *mos* gene. J. Virol. **56:**144–152.
50. **Shibuya, E. K., and J. V. Ruderman.** 1993. Mos induces the *in vitro* activation of mitogen-activated protein kinases in lysates of frog oocytes and mammalian somatic cells. Mol. Biol. Cell **4:**781–790.
51. **Singh, B.** Unpublished data.
52. **Singh, B., F. Al-Bagdadi, J. Liu, and R. B. Arlinghaus.** 1990. Use of anti-peptide antibodies to probe the catalytic activity of $p37^{v\text{-}mos}$. Virology **178:** 535–542.
53. **Singh, B., and R. B. Arlinghaus.** 1989. Vimentin phosphorylation by $p37^{mos}$ protein kinase *in vitro* and generation of 50 kDa cleavage product in v-*mos* transformed cells. Virology **173:**144–156.
54. **Singh, B., and R. B. Arlinghaus.** 1992. The *mos* proto-oncogene product: its role in oocyte maturation, metaphase arrest and neoplastic transformation. Mol. Carcinog. **6:**182–189.
55. **Singh, B., M. Hannink, D. J. Donoghue, and R. B. Arlinghaus.** 1986. $p37^{mos}$ associated serine/threonine protein kinase activity correlates with the cellular transformation function of v-*mos*. J. Virol. **60:**1148–1152.
56. **Singh, B., N. K. Herzog, J. Liu, and R. B. Arlinghaus.** 1988. $p37^{mos}$ encoded by the HT-1 strain of Moloney murine sarcoma virus has an associated protein kinase activity. Oncogene **3:**79–85.
57. **Singh, B., C. Stocking, R. Walker, Y. Yang, W. Ostertag, and R. B. Arlinghaus.** 1992. v-Mos proteins encoded by myeloproliferative sarcoma virus and its *ts*159 mutant. J. Virol. **66:**1267–1272.
58. **Singh, B., C. Wittenberg, M. Hannink, S. I. Reed, D. J. Donoghue, and R. B. Arlinghaus.** 1988. The histidine-221 to tyrosine substitution in v-Mos abolishes its biological function and its protein kinase activity. Virology **164:** 114–120.
59. **Songyang, Z., S. Blechner, N. Hoagland, M. F. Hoekstra, H. Piwnica-Worms, and L. C. Cantley.** 1994. Use of an oriented peptide library to determine the optimal substrates of protein kinases. Curr. Biol. **4:**973–982.
60. **Urner, R., W. L. Hermann, E. E. Balieu, and S. Schorderet-Slatkine.** 1983. Inhibition of denuded mouse oocyte meiotic maturation by forskolin, an activator of adenylate cyclase. Endocrinology **113:**1170–1172.
61. **van Beveren, C., F. van Straaten, J. A. Galleshaw, and I. M. Verma.** 1981. Nucleotide sequence of the genome of a murine sarcoma virus. Cell **27:** 97–108.
62. **Yang, Y., R. B. Arlinghaus, and B. Singh.** Unpublished data.
63. **Zhao, X., B. Batten, B. Singh, and R. B. Arlinghaus.** 1990. Requirement of the c-*mos* protein kinase for murine meiotic maturation. Oncogene **5:**1727–1730.
64. **Zhao, X., B. Singh, and R. B. Arlinghaus.** 1991. Inhibition of c-*mos* protein kinase blocks mouse zygotes at the pronuclei stage. Oncogene **6:**1423–1426.
65. **Zhou, R., M. Oskarsson, R. S. Paules, N. Schulz, D. Cleveland, and G. F. Vande Woude.** 1991. Ability of the c-*mos* product to associate with and phosphorylate tubulin. Science **251:**671–675.